

1 **Long term variations of river temperature and the influence of atmospheric**
2 **and hydrological factors: case study of Kupa River watershed in Croatia**

3 Senlin Zhu^{1*}, Ognjen Bonacci², Dijana Oskoruš³, Marijana Hadzima-Nyarko⁴

4 ¹State Key Laboratory of Hydrology-Water resources and Hydraulic Engineering, Nanjing
5 Hydraulic Research Institute, Nanjing 210029, China; ORCID: 0000-0001-7561-8372

6 ²Faculty of Civil Engineering and Architecture, University of Split, Matice hrvatske 15, 21000
7 Split, Croatia

8 ³Meteorological and Hydrological Service, Zagreb, Croatia

9 ⁴Faculty of Civil Engineering Osijek, University J.J. Strossmayer in Osijek, Osijek, Croatia

10 *Corresponding author: slzhu@nhri.cn, +86 159-2637-0451

11
12
13 **Abstract**

14 Long term variations of river water temperatures (RWT) in Kupa River watershed, Croatia were
15 investigated. It is shown that the RWT in the studied river stations increased about 0.0232-0.0796
16 °C per year, which are comparable with long term observations reported for rivers in other regions,
17 indicating an apparent warming trend. RWT rises during the past 20 years have not been constant
18 for different periods of the year, and the contrasts between stations regarding RWT increases vary
19 seasonally. Additionally, multilayer perceptron neural network models (MLPNN) and adaptive
20 neuro-fuzzy inference systems (ANFIS) models were implemented to simulate daily RWT, using
21 air temperature (T_a), flow discharge (Q) and the day of year (DOY) as predictors. Results showed
22 that compared to the individual variable alone with T_a as input, combining T_a and Q in the MLPNN

23 and ANFIS models explained temporal variations of daily RWT more accurately. Including of the
24 three inputs as predictors (T_a , Q and the DOY) yielded the best accuracy among all the developed
25 models. Modeling results indicate that the developed models can well reproduce the seasonal
26 dynamics of RWT in each river, and the models may be used for future projections of RWT by
27 coupling with regional climate models.

28 Keywords: air temperature, climate change, flow discharge, machine learning models, river water
29 temperature

30

31 **Introduction**

32 River water temperature (RWT) is one of the most important indicators to determine the overall
33 health of aquatic ecosystems since it affects various physical and biochemical processes in rivers
34 (Rice & Jastram 2015). For example, RWT significantly impacts dissolved oxygen dynamics (Cox
35 & Whitehead 2009), the formation of potentially toxic ammonia (Kim *et al.* 2017), and the evolution
36 and distribution of aquatic organisms (Fullerton *et al.* 2018). Cingi *et al.* (2010) stressed that
37 relatively small increases in RWT during the spawning period of *Coregonus lavaretus* may lead to
38 fatal impacts on its recruitment and population persistence.

39 Understanding the factors impacting RWT and how thermal regimes have changed in the past
40 and how they can be modified in the future is therefore of great significance for the sustainable
41 management of river ecosystems. This is especially important in recent decades considering the
42 rising of air temperatures due to climate change (van Vliet *et al.* 2013; DeWeber & Wagner 2014),
43 the impacts of extreme climate events such as heatwaves (Feng *et al.* 2018) and anthropogenic
44 activities such as land use change (DeWeber & Wagner 2014), urbanization (DeWeber & Wagner

45 2014; Chen *et al.* 2016) and damming (Ayllón *et al.* 2012). Rising RWT is strongly related to climate
46 warming with various time scales for different type of rivers, which have been reported in a lot of
47 studies (Webb *et al.* 2003; Bonacci *et al.* 2008; Chen *et al.* 2016) since air temperature is a major
48 component in calculating net heat fluxes at the air-water interface. For example, Chen *et al.* (2016)
49 indicated that RWT in the Yongan watershed increased by 0.029–0.046 °C year⁻¹ due to a ~0.050 °C
50 year⁻¹ increase of air temperature over the 1980–2012 period. Depending on the river type and time
51 scale, the air-water temperature relationships can be explained by linear or logistic functions (Webb
52 *et al.* 2003), machine learning models (DeWeber & Wagner 2014; Piotrowski *et al.* 2015; Zhu *et al.*
53 2018), and hybrid statistically and physically based models (Toffolon & Piccolroaz 2015).

54 Although the air-water temperature relationship is generally strong, the strength of such a
55 relationship varies regionally and temporally, and can be highly site specific due to additional
56 influences from local hydrology and human activities (DeWeber & Wagner 2014; Zhu *et al.* 2018).
57 It is commonly observed that RWT is inversely related to river discharge, and a global assessment
58 indicated that a decrease in river discharge by 20% and 40% would exacerbate water temperature
59 increases by 0.3 °C and 0.8 °C on average, respectively (van Vliet *et al.* 2011). Additionally, it was
60 found that flow discharge played a relevant role mainly in snow-fed and regulated rivers with higher
61 altitude hydropower reservoirs, while it played a minor role in lowland rivers for RWT dynamics
62 (Zhu *et al.* 2018).

63 Kupa River watershed is one of the most important water resources in Croatia. Since river
64 thermal conditions impact various processes in river systems, such as dissolved oxygen
65 concentrations and water quality status, thus, quantifying thermal dynamics in this particular river
66 catchment is of great significance to water resources managers. Previously, Bonacci *et al.* (2008)

67 analyzed water temperature regime of the Danube and its tributaries in Croatia. In their research,
68 water temperature data in the main stem of the Kupa River was used. However, the RWT data from
69 the main stem hydrological stations were only limited to 1951-2003. In this study, the latest RWT
70 and flow discharge data from 6 hydrological stations on the main tributaries of Kupa River were
71 used to evaluate the thermal regime for the watershed. The multilayer perceptron neural network
72 (MLPNN) and adaptive neuro-fuzzy inference system (ANFIS) models developed for the Drava
73 River (Zhu *et al.* 2018) were used to quantify the impact of air temperature and flow discharge on
74 RWT dynamics. The research will help to inform water resources management in Croatia.

75 **Materials and methods**

76 **Study area**

77 The study covers the Kupa River basin, situated between Croatia (86% of total basin area) and
78 Slovenia (14% of total basin area) in the hinterland of the Northern Adriatic Sea partly as Dinaric
79 karst terrain in upper part of the basin. The basin is rather small, but abounds in high quality water,
80 and is partly located at a higher altitude. This is a typical example of complex karst
81 hydrological/hydrogeological behavior, located in the north-western part of the deep and developed
82 Croatian Dinaric karst, due to which the hydrological drainage area is not strongly defined (Bonacci
83 & Andrić 2010). Continental climate mixes with Mediterranean climate influence in upper part of
84 the basin, while in lower part, Pannonian climate is the most important. As a river of multifarious
85 applied potential, the patterns of land use in the Kupa River basin include mountains (26%), forests
86 (33%), pasture (26%) and agriculture (15%). Hydrological parameters (water temperature and flow
87 discharge) were regularly monitored at several gauging stations in the Kupa River watershed.
88 Considered the data availability, six gauging stations in the Kupa River watershed were selected

89 (Fig. 1). Table 1 presents the main characteristics of the 6 studied gauging stations (station name,
 90 station elevation, drainage area, period of available data for water temperature and flow discharge).
 91 Monitoring of water temperature is based on a once-daily measurement at 7.30 am in Croatia. Air
 92 temperatures (T_a) were obtained from the nearby meteorological station in Ogulin (Fig. 1). Daily
 93 averaged T_a was in the period 1990-2017.

94

95 **Figure 1** Location maps indicating (a) the study area and (b) schematic presentation of the 6
 96 gauging stations and corresponding meteorological station

97

98 **Table 1** Main characteristics of the 6 studied water temperature gauging stations in the Kupa

99

River watershed				
River name	Station name	Elevation (m a.s.l.)	Drainage area (km ²)	Period of available data
Čabranka	Zamost 2	297.540	134.451 ^a	$T_w Q$: 1990-1999 2002-2008
Donja Dobra	Stative Donje	116.456	49.344 ^a	$T_w Q$: 1994-2017
Donja Mrežnica	Mrzlo Polje	113.967	257.953 ^a	$T_w Q$: 1990-2017
Gornja Dobra	Luke	353.668	162.00 ^b	$T_w Q$: 1991-1992 1994-2015
Korana	Slunj Uzvodni	212.167	572.341 ^a	$T_w Q$: 1996-2004 2007-2017
Slunjčica	Rastoke	226.899	273.00 ^b	$T_w Q$: 1996-2017

100 T_w : water temperature; Q : flow discharge; a Hydrological drainage area, b Topographical drainage area

101

102 Machine learning models

103 In the present study, the MLPNN and ANFIS models developed previously (Zhu *et al.* 2018)

104 were used. For the MLPNN model, the weights (w_{ij}) and bias levels (δ_o) are the only parameters that

105 need to be adjusted when the structure of the neural network has been defined (number of layers,

106 number of neurons in each layer, activation function for each layer). Modification of these

107 parameters will change the output values of the designed network. The weights (w_{ij}) and bias levels

108 (δ_o) need to be adjusted to minimize the modeling error. The root mean squared error (RMSE) and

109 the mean squared error (MSE) is often used to define the network error. In this study, the MLPNN

110 model has one hidden layer with sigmoidal activation function, and one output layer with linear

111 activation function. The number of neurons in the hidden layer varies from one station to another,
112 however, in the major part of the present investigation the number was generally between 10 and
113 13. To develop ANFIS model, it is important to create the fuzzy rule base. The number of fuzzy
114 rule for any ANFIS model is directly related to the identification method used for partitioning the
115 input space. According to the previous research results (Zhu *et al.* 2018), the fuzzy c-means
116 clustering (FC) was used. When using FC method, the number of fuzzy rules is equal to the clusters
117 and fixed by the user. Detailed information about the two models can be found in Zhu *et al.* (2018).

118 In this study, both the scripts of the MLPNN and ANFIS models were implemented in Matlab.
119 Besides air temperature (T_a) and flow discharge (Q), the day of the year (DOY) was also used as
120 input variable. The MLPNN and ANFIS models were developed according to the following three
121 different versions: (i) version 1 with only one input variable (T_a), (ii) version 2 with two inputs
122 variable (T_a and Q) and (iii) version 3 with three inputs (T_a , Q and the DOY). For the six river
123 stations, data period for model calibration and validation are respectively: (1) 1990-1999 and 2002-
124 2008 for Čabranka River, (2) 1994-2009 and 2010-2017 for Donja Dobra River, (3) 1990-2007 and
125 2008-2017 for Donja Mrežnica River, (4) 1991-1992 plus 1994-2007 and 2008-2015 for Gornja
126 Dobra River, (5) 1996-2004 plus 2008-2010 and 2011-2017 for Korana River, and (6) 1996-2009
127 and 2010-2017 for Slunjčica River.

128 **Model evaluation metrics**

129 Model performances were evaluated using the following four indicators (Zhu *et al.* 2018): the
130 coefficient of correlation (R), the Willmott index of agreement (d), the root mean squared error
131 (RMSE), and the mean absolute error (MAE).

$$R = \left[\frac{\frac{1}{n} \sum_{i=1}^n (O_i - O_m)(P_i - P_m)}{\sqrt{\frac{1}{n} \sum_{i=1}^n (O_i - O_m)^2} \sqrt{\frac{1}{n} \sum_{i=1}^n (P_i - P_m)^2}} \right] \quad (1)$$

$$d = 1 - \frac{\sum_{i=1}^n (P_i - O_i)^2}{\sum_{i=1}^n (|P_i - O_m| + |O_i - O_m|)^2} \quad (2)$$

$$RMSE = \sqrt{\frac{1}{n} \sum_{i=1}^n (O_i - P_i)^2} \quad (3)$$

$$MAE = \frac{1}{n} \sum_{i=1}^n |O_i - P_i| \quad (4)$$

132 where n is the number of data samples, O_i is the observed and P_i is the predicted water temperatures.

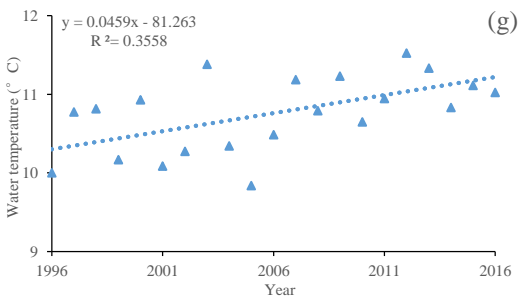
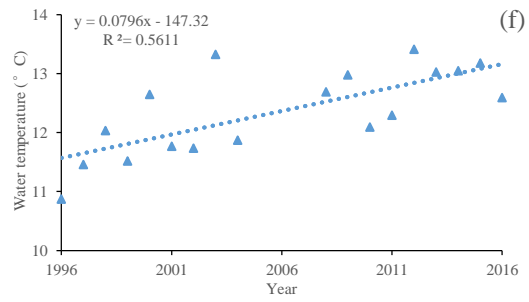
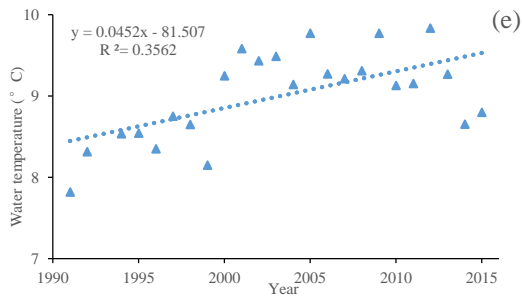
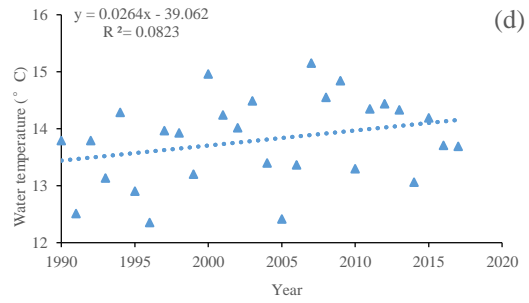
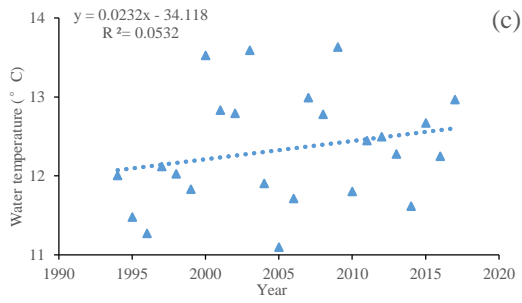
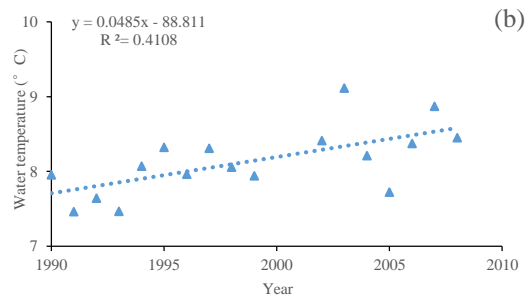
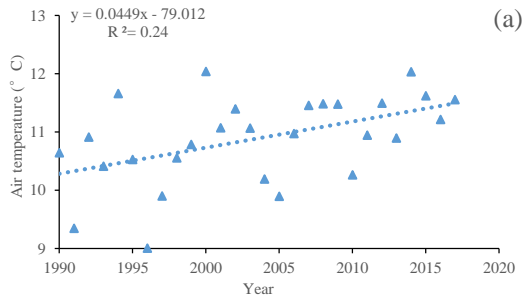
133 O_m and P_m are the average values of O_i and P_i .

134 **Results and discussion**

135 **Dynamic variations of water temperature and air temperature**

136 The annual variations of T_a and T_w are presented in Fig. 2. It is shown that the air temperatures
 137 presented an increasing trend about $0.0449 \text{ } ^\circ\text{C year}^{-1}$, indicating an apparent warming trend. The
 138 increases of RWT differ between the studied river stations, and the RWT increase rate ($^\circ\text{C year}^{-1}$)
 139 negatively correlated with annual averaged flow discharge (Fig. 3). RWT increased about 0.0232 -
 140 $0.0796 \text{ } ^\circ\text{C per year}$, which is comparable with long term observations reported for rivers in China
 141 (0.029 - $0.046 \text{ } ^\circ\text{C year}^{-1}$, [Chen et al. 2016](#)), USA (0.009 - $0.077 \text{ } ^\circ\text{C year}^{-1}$, [Isakk et al. 2012](#); [van Vliet](#)
 142 [et al. 2013](#); [Rice & Jastram 2015](#)) and Europe (0.006 - $0.18 \text{ } ^\circ\text{C year}^{-1}$, [Moatar & Gailhard 2006](#); [Albek](#)
 143 [& Albek 2009](#); [Pekárová et al. 2011](#); [Žganec et al. 2012](#); [Markovic et al. 2013](#); [Lepori et al. 2014](#);
 144 [Orr et al. 2015](#); [Hardenbicker et al. 2017](#)).

145



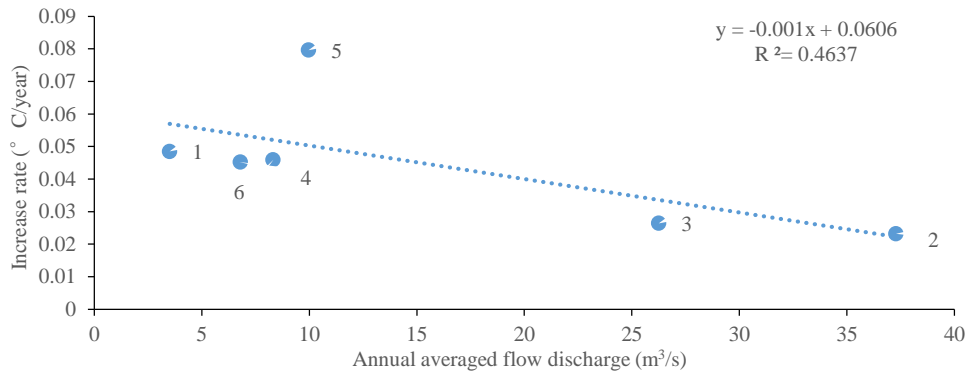
146

147

148

149

150 **Figure 2** Annual variations of T_a and T_w : (a) T_a in Ogulin, (b) T_w in Čabranka, (c) T_w in Donja
 151 Dobra, (d) T_w in Donja Mrežnica, (e) T_w in Gornja Dobra, (f) T_w in Korana and (g) T_w in Slunjčica
 152



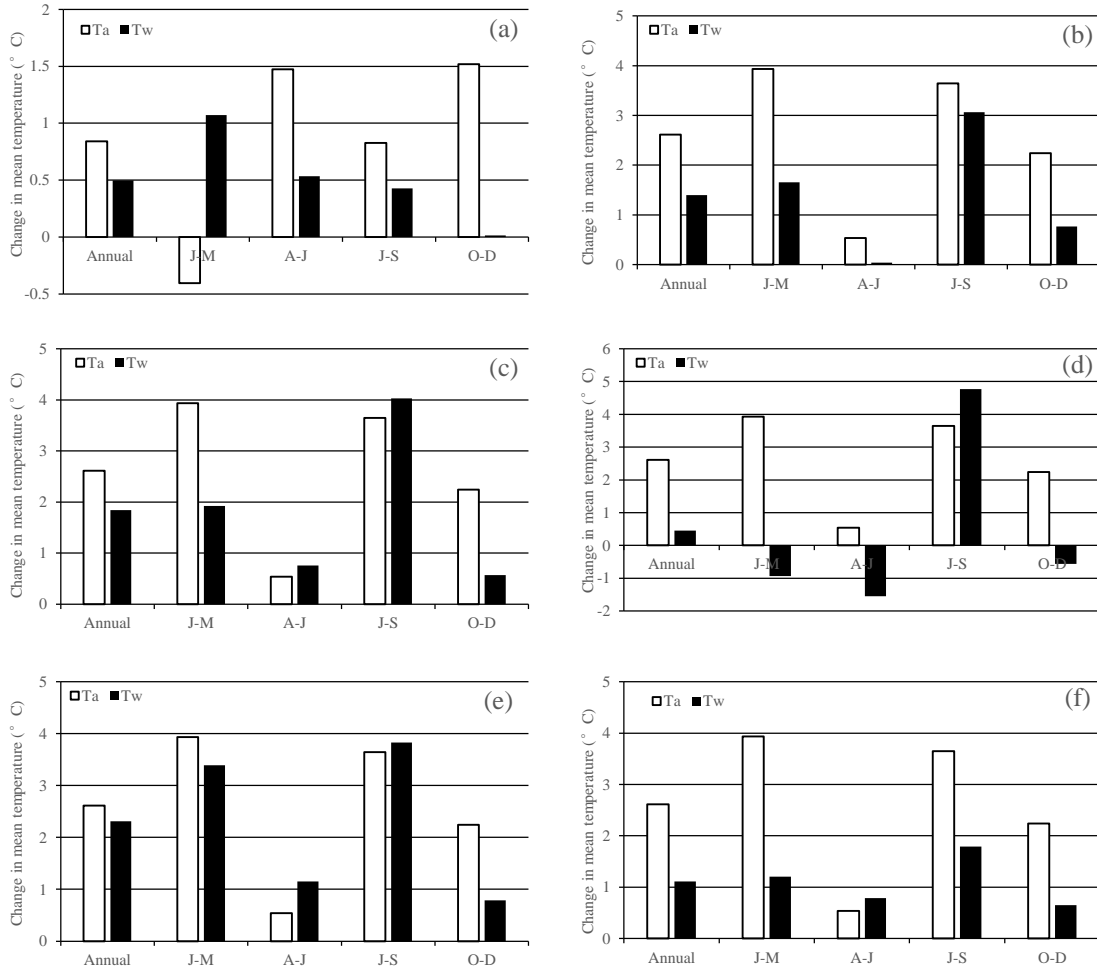
153

154 **Figure 3** Linear relationship between increase rate of river temperature and annual averaged flow
 155 discharge for the six river stations (1-Čabranka, 2-Donja Dobra, 3-Donja Mrežnica, 4-Gornja
 156 Dobra, 5-Korana, 6- Slunjčica)

157

158 Fig. 4 presented changes in T_a and T_w between 1996 and 2015 for annual and seasonal average
 159 values. Since the Čabranka River only has data till 2008, data from 1990 and 2008 was compared.
 160 It is shown in Fig. 4 that in the past 20 years (1996-2015), with an increase of 2.613 °C for air
 161 temperature, the annual mean of RWT increased about 0.45-2.308 °C. Increases in annual mean
 162 RWT was highest for the Korana River and least for the Gornja Dobra River. Repeating this analysis
 163 for different seasonal quarters revealed that RWT rises during the past 20 years have not been
 164 constant for different periods of the year, and the contrasts between river stations regarding RWT
 165 increases vary seasonally. For the Čabranka river (Fig. 4(a)), though air temperature in January-
 166 March decreased, RWT in different seasons still increased between 0.013 and 1.07 °C. For the other
 167 five rivers, the greatest rises in average RWT were in July–September period (1.789-4.767 °C).
 168 Particularly, in the Korana River (Fig. 4(e)), RWT increases in January–March and July–September
 169 exceeded 3.0 °C. Except for the Gornja Dobra River, RWT in different seasons for all the other four
 170 rivers increased with the increase of air temperature (Fig. 4(b)-(f)).

171



172

173

174

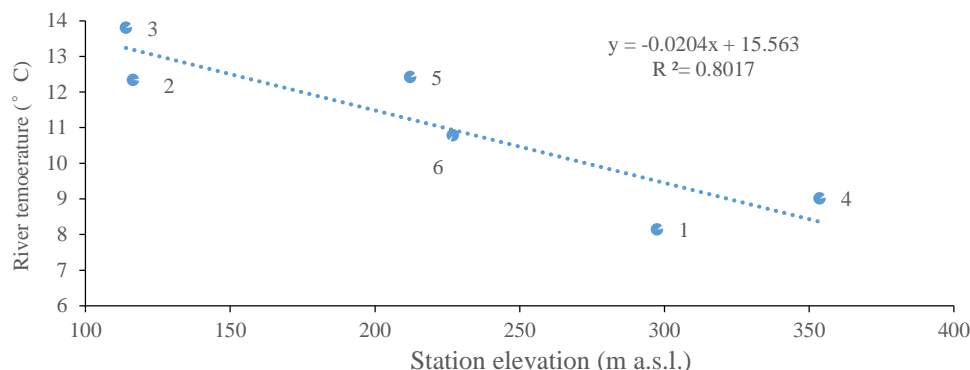
175 **Figure 4** Changes in T_a and T_w between 1996 and 2015 for annual and seasonal average values (J-
 176 M: January–March; A-J: April–June; J-S: July–September; O-D: October–December): (a)
 177 Čabranka (between 1990 and 2008), (b) Donja Dobra, (c) Donja Mrežnica, (d) Gornja Dobra, (e)
 178 Korana, (f) Slunjčica

179

180 Fig. 5 presents a linear relationship between the mean annual RWT and the station elevation
 181 for the six river stations. Results showed that the mean annual RWT negatively correlated with
 182 station elevation, which is consistent with previous analysis for river stations in the main stem of
 183 the Kupa River (Bonacci *et al.* 2008). However, the mean annual RWT presented no significant
 184 correlation with the drainage area listed in Table 1, which may be explained by that the Kupa River
 185 watershed is a typical example of complex karst hydrological/hydrogeological behavior and the

186 hydrological drainage area is not strongly defined (Bonacci & Andrić 2010).

187



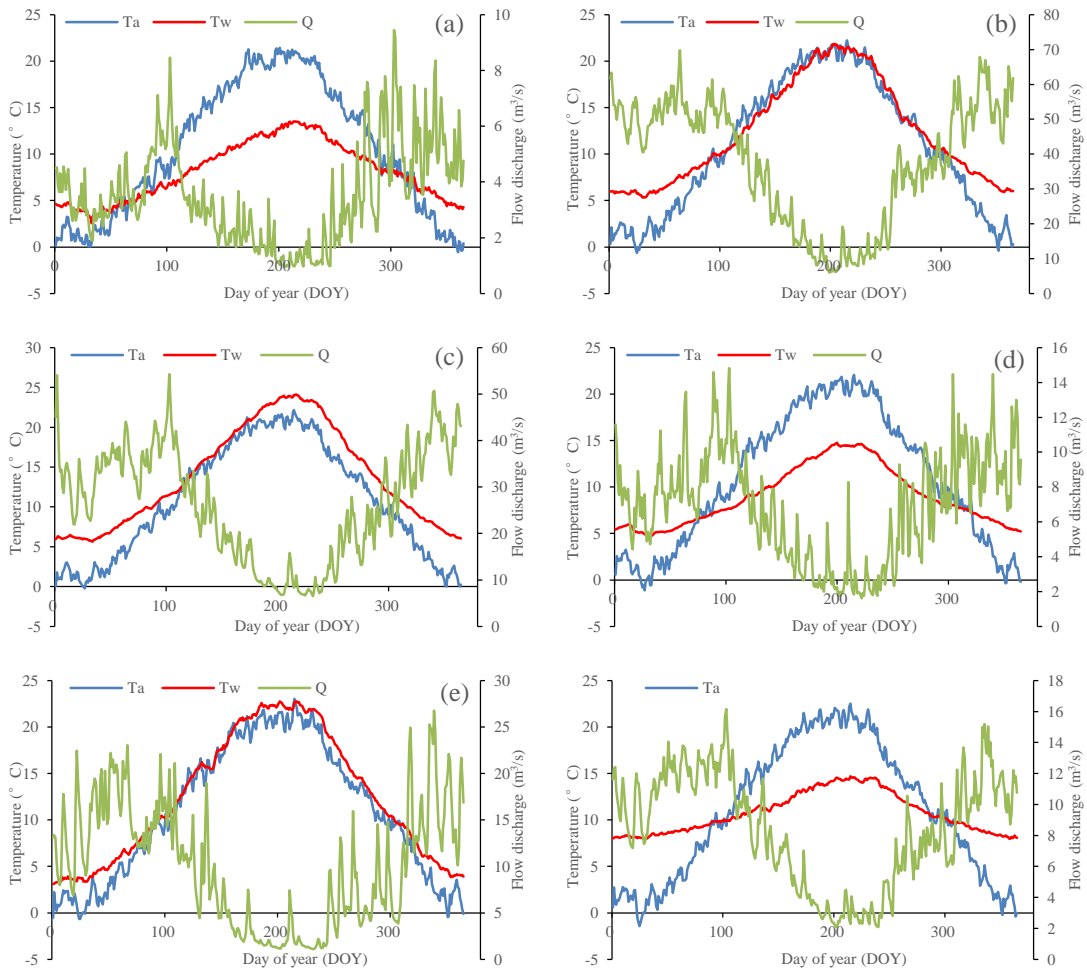
188

189 **Figure 5** Linear relationship between mean annual river temperature and station elevation for the
190 six river stations (1-Čabranka, 2-Donja Dobra, 3-Donja Mrežnica, 4-Gornja Dobra, 5-Korana, 6-
191 Slunjčica)

192

193 The seasonal dynamics of water temperature (T_w), air temperature (T_a) and flow discharge (Q)
194 are presented in Fig. 6 through the climatological year, which is defined by averaging for each day
195 of the year all measurements available over the observation period for that same specific day (Zhu
196 *et al.* 2018). Generally, river flow mainly distributed in the spring and winter period for the six
197 rivers, at which time the air and water temperatures are lower. However, for the high temperature
198 period, especially for summer, flow discharge is generally small, which may further intensify RWT
199 increases. The response of T_w to changes in T_a is almost linear for the Donja Dobra River (Fig. 6(b)),
200 the Donja Mrežnica River (Fig. 6(c)) and Korana River (Fig. 6(e)). Typically for the Donja Mrežnica
201 River (Fig. 6(c)), T_w in the climatological year were larger than T_a all the year round. The Čabranka
202 River (Fig. 6(a)), Gornja Dobra River (Fig. 6(d)), and Slunjčica River (Fig. 6(f)) presented a clear
203 flattening of the seasonal pattern of T_w , especially in summer.

204



205

206

207

208 **Figure 6** Climatological (reference) year for the six river stations: (a) Čabranka, (b) Donja Dobra,
209 (c) Donja Mrežnica, (d) Gornja Dobra, (e) Korana, (f) Slunjčica

210

211 Machine learning models for modeling daily river water temperature

212 Considering the influences of T_a , Q and the seasonal component (DOY), the MLPNN and
213 ANFIS models were developed for daily RWT for each river station. Modeling performance was
214 summarized in Table 2. The two models performed comparatively with MLPNN model performed
215 slightly better, conforming the previous conclusion of [Zhu et al. \(2018\)](#). Compared to the individual
216 variable alone (version 1 with T_a as input), combining T_a and Q in the MLPNN and ANFIS models
217 (version 2) explained temporal variations of daily RWT more accurately (Table 3), especially for

218 the Donja Dobra, Donja Mrežnica and Slunjčica rivers. For example, for the Slunjčica River, the
219 MLPNN2 model decreased the RMSE and MAE values of MLPNN1 by 25.90% and 26.97% in the
220 calibration phase, and 14.97% and 17.48% in the validation phase. The predictive capability was
221 further improved by combining T_a , Q and DOY (Table 3). By including DOY as model input,
222 modeling performances dramatically improved (Table 3), which indicates that the seasonal
223 component DOY plays an important role for RWT forecasting. For the Donja Mrežnica River, the
224 ANFIS3 model decreased the RMSE and MAE values of ANFIS1 by 57.35% and 57.79% in the
225 calibration phase, and 57.20% and 57.24% in the validation phase. Generally, the two models
226 performed well for RWT predictions. For model version 3, R and d values varied between 0.916
227 and 0.98, and 0.954 and 0.99 respectively in the calibration phase, and RMSE and MAE values
228 ranged from 0.767 to 1.603, and 0.58 to 1.258. In the validation phase, R and d values varied
229 between 0.907 and 0.978, and 0.951 and 0.989 respectively, and RMSE and MAE values ranged
230 from 0.872 to 1.793, and 0.627 to 1.435. The modeling performances are comparable with that for
231 the two river stations in the Drava River with RMSE varying between 1.227 and 1.69, MAE varying
232 between 0.956 and 1.337 (Zhu *et al.* 2018). Fig. 7 shows the variation of annual RMSE values
233 (MLPNN3) for the whole modeling period in each river. Results indicate that the annual RMSE
234 values varied between years, and generally the model performed well with low RMSE values. Fig.
235 8 presents the modeling performances of the MLPNN3 for the climatological year at the six river
236 stations. As is shown, the MLPNN3 model can well reproduce the seasonal dynamics of RWT in
237 each river.

238

239

240

241

242

243

244

245

246

247 **Table 2** Performances of different models in modelling water temperature (T_w °C) for the studied
 248 rivers in the Kupa River watershed

River name	Model version	Training (Calibration)				Validation			
		<i>R</i>	<i>d</i>	<i>RMSE</i> (°C)	<i>MAE</i> (°C)	<i>R</i>	<i>d</i>	<i>RMSE</i> (°C)	<i>MAE</i> (°C)
Čabranka	MLPNN3	0.956	0.977	0.986	0.774	0.941	0.970	1.262	0.979
	MLPNN2	0.916	0.955	1.342	1.037	0.908	0.953	1.585	1.242
	MLPNN1	0.882	0.934	1.576	1.261	0.884	0.937	1.715	1.370
	ANFIS3	0.954	0.976	1.005	0.787	0.943	0.971	1.233	0.965
	ANFIS2	0.918	0.956	1.330	1.020	0.908	0.953	1.571	1.230
	ANFIS1	0.882	0.934	1.577	1.261	0.887	0.938	1.699	1.361
Donja Dobra	MLPNN3	0.972	0.986	1.406	1.047	0.964	0.982	1.460	1.083
	MLPNN2	0.935	0.966	2.118	1.545	0.919	0.957	2.167	1.619
	MLPNN1	0.890	0.939	2.724	2.061	0.874	0.931	2.659	2.040
	ANFIS3	0.972	0.985	1.416	1.056	0.963	0.981	1.469	1.088
	ANFIS2	0.935	0.966	2.117	1.544	0.918	0.956	2.174	1.630
	ANFIS1	0.891	0.940	2.721	2.060	0.873	0.930	2.673	2.048
Donja Mrežnica	MLPNN3	0.980	0.990	1.274	0.990	0.978	0.989	1.334	1.040
	MLPNN2	0.923	0.959	2.479	1.828	0.923	0.959	2.450	1.801
	MLPNN1	0.882	0.934	3.042	2.374	0.873	0.930	3.115	2.417
	ANFIS3	0.980	0.990	1.297	1.002	0.978	0.989	1.334	1.034
	ANFIS2	0.923	0.959	2.476	1.828	0.923	0.959	2.453	1.798
	ANFIS1	0.882	0.934	3.041	2.374	0.873	0.930	3.117	2.418
Gornja Dobra	MLPNN3	0.919	0.956	1.225	0.925	0.907	0.951	1.724	1.361
	MLPNN2	0.852	0.915	1.630	1.200	0.823	0.901	2.323	1.838
	MLPNN1	0.839	0.906	1.693	1.265	0.794	0.884	2.492	1.874
	ANFIS3	0.916	0.954	1.251	0.948	0.907	0.951	1.716	1.377
	ANFIS2	0.852	0.915	1.630	1.198	0.824	0.902	2.316	1.830
	ANFIS1	0.838	0.906	1.696	1.267	0.814	0.894	2.364	1.858
Korana	MLPNN3	0.975	0.987	1.552	1.222	0.969	0.982	1.763	1.408
	MLPNN2	0.932	0.964	2.537	1.933	0.917	0.950	2.831	2.227
	MLPNN1	0.915	0.954	2.823	2.175	0.904	0.949	2.960	2.322
	ANFIS3	0.974	0.986	1.603	1.258	0.968	0.982	1.793	1.435
	ANFIS2	0.933	0.964	2.530	1.933	0.917	0.951	2.823	2.200
	ANFIS1	0.915	0.954	2.823	2.175	0.904	0.949	2.961	2.324
Slunjčica	MLPNN3	0.952	0.975	0.767	0.580	0.938	0.956	0.882	0.655
	MLPNN2	0.922	0.958	0.967	0.715	0.909	0.939	1.028	0.765
	MLPNN1	0.853	0.915	1.305	0.979	0.851	0.920	1.209	0.927
	ANFIS3	0.951	0.974	0.771	0.582	0.939	0.957	0.872	0.627
	ANFIS2	0.922	0.958	0.965	0.715	0.909	0.939	1.024	0.764
	ANFIS1	0.853	0.915	1.305	0.978	0.852	0.920	1.208	0.926

249

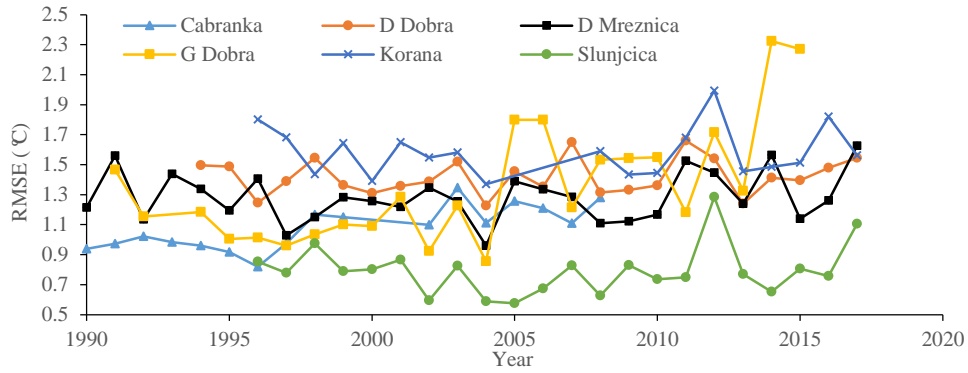
250

251 **Table 3** Percentage difference in modelling performance between models version 3 and 2
 252 relative to model version 1 ($\Delta X_i = (X_i - X_1) / X_1 * 100$, where X is the generic model performance
 253 metric and the subscript i indicates either model MLPNN2/ANFIS2 ($i=2$) or model
 254 MLPNN3/ANFIS3 ($i=3$))

River name	Model	ΔX_i	Training (Calibration)				Validation			
			ΔR	Δd	$\Delta RMSE$	ΔMAE	ΔR	Δd	$\Delta RMSE$	ΔMAE
Čabranka	MLPNN	ΔX_3	8.39	4.60	-37.44	-38.62	6.45	3.52	-26.41	-28.54
		ΔX_2	3.85	2.25	-14.85	-17.76	2.71	1.71	-7.58	-9.34
	ANFIS	ΔX_3	8.16	4.50	-36.27	-37.59	6.31	3.52	-27.43	-29.10
		ΔX_2	4.08	2.36	-15.66	-19.11	2.37	1.60	-7.53	-9.63
Donja Dobra	MLPNN	ΔX_3	9.21	5.01	-48.38	-49.20	10.30	5.48	-45.09	-46.91
		ΔX_2	5.06	2.88	-22.25	-25.04	5.15	2.79	-18.50	-20.64
	ANFIS	ΔX_3	9.09	4.79	-47.96	-48.74	10.31	5.48	-45.04	-46.88
		ΔX_2	4.94	2.77	-22.20	-25.05	5.15	2.80	-18.67	-20.41
Donja Mrežnica	MLPNN	ΔX_3	11.11	6.00	-58.12	-58.30	12.03	6.34	-57.17	-56.97
		ΔX_2	4.65	2.68	-18.51	-23.00	5.73	3.12	-21.35	-25.49
	ANFIS	ΔX_3	11.11	6.00	-57.35	-57.79	12.03	6.34	-57.20	-57.24
		ΔX_2	4.65	2.68	-18.58	-23.00	5.73	3.12	-21.30	-25.64
Gornja Dobra	MLPNN	ΔX_3	9.54	5.52	-27.64	-26.88	14.23	7.58	-30.82	-27.37
		ΔX_2	1.55	0.99	-3.72	-5.14	3.65	1.92	-6.78	-1.92
	ANFIS	ΔX_3	9.31	5.30	-26.24	-25.18	11.43	6.38	-27.41	-25.89
		ΔX_2	1.67	0.99	-3.89	-5.45	1.23	0.89	-2.03	-1.51
Korana	MLPNN	ΔX_3	6.56	3.46	-45.02	-43.82	7.19	3.48	-40.44	-39.36
		ΔX_2	1.86	1.05	-10.13	-11.13	1.44	0.11	-4.36	-4.09
	ANFIS	ΔX_3	6.45	3.35	-43.22	-42.16	7.08	3.48	-39.45	-38.25
		ΔX_2	1.97	1.05	-10.38	-11.13	1.44	0.21	-4.66	-5.34
Slunjčica	MLPNN	ΔX_3	11.61	6.56	-41.23	-40.76	10.22	3.91	-27.05	-29.34
		ΔX_2	8.09	4.70	-25.90	-26.97	6.82	2.07	-14.97	-17.48
	ANFIS	ΔX_3	11.49	6.45	-40.92	-40.49	10.21	4.02	-27.81	-32.29
		ΔX_2	8.09	4.70	-26.05	-26.89	6.69	2.07	-15.23	-17.49

255

256

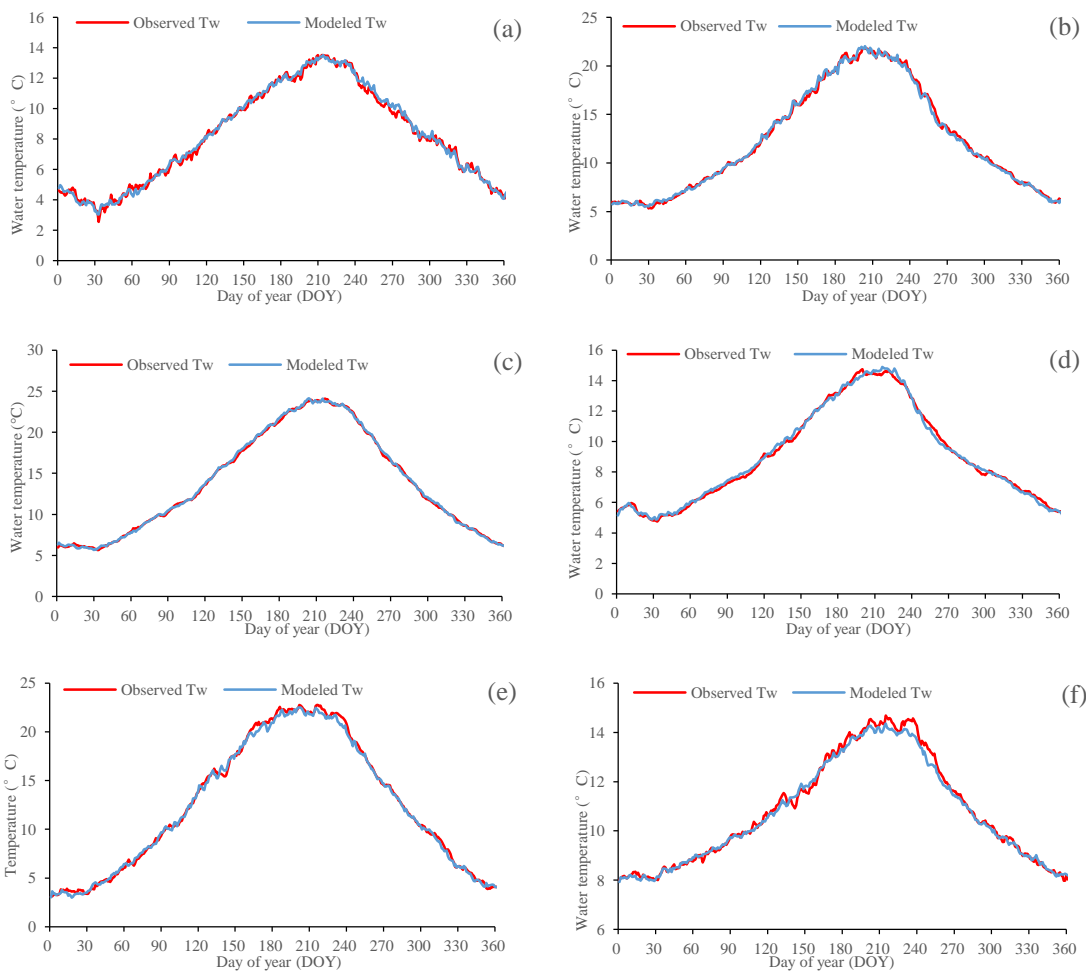


257

258

Figure 7 Variation of annual RMSE values for the MLPNN3 models

259



260

261

262

263

Figure 8 Modeling performances of the MLPNN3 for the climatological year at the six river

264

stations: (a) Čabranka, (b) Donja Dobra, (c) Donja Mreznica, (d) Gornja Dobra, (e) Korana, and

265

(f) Slunjčica

266

267

Conclusions

268 In this study, long term changes of RWT from six river stations in Kupa River watershed,
269 Croatia were investigated. Results showed that RWT in the six studied river stations increased about
270 0.0232-0.0796 °C per year with an increasing trend of air temperatures about 0.0449 °C year⁻¹,
271 indicating an apparent warming trend. The results are comparable with long term observations for
272 rivers in other regions (China, USA and Europe etc.). With an increase of 2.613 °C for air
273 temperature, the annual mean of RWT increased about 0.45-2.308 °C in the past 20 years (1996-
274 2015). Results for different seasonal quarters revealed that temperature rises during the past 20 years
275 have not been constant for different periods of the year, and the contrasts between stations regarding
276 temperature increases vary seasonally. In addition, MLPNN and ANFIS models were developed to
277 predict daily RWT, using T_a , Q and DOY as model inputs. Results showed that compared to the
278 model version 1 with T_a as input, model version 2 by combining T_a and Q better explained temporal
279 variations of daily RWT. Using the three inputs as predictors (T_a , Q and the DOY) yielded the best
280 accuracy among all the developed models. For model version 3, RMSE and MAE values ranged
281 from 0.767 to 1.603, and 0.58 to 1.258 in the calibration phase, and in the validation phase, RMSE
282 and MAE values varied from 0.872 to 1.793, and 0.627 to 1.435 respectively. Modeling results
283 indicate that the developed models can well reproduce the seasonal dynamics of RWT. For further
284 research, the models can be coupled with regional climate models for future projections of RWT.

285 **Acknowledgements**

286 We acknowledge the Croatian Meteorological and Hydrological Service for providing the
287 water temperature, air temperature and river flow discharge data used in this study. This work was
288 jointly funded by the National Key R&D Program of China (2018YFC0407203, 2016YFC0401506),
289 China Postdoctoral Science Foundation (2018M640499) and the research project from Nanjing

290 Hydraulic Research Institute (Y118009).

291 **References**

292 Albek, M. & Albek, E. 2009 Stream temperature trends in Turkey. *Clean Soil Air & Water*, **37**(2),
293 142-149.

294 Ayllón, D., Almodóvar, A., Nicola, G. G., Parra, I. & Elvira, B. 2012 A new biological indicator to
295 assess the ecological status of Mediterranean trout type streams. *Ecological Indicators*, **20**(3),
296 295-303.

297 Bonacci, O. & Andrić, I. 2010 Impact of an inter - basin water transfer and reservoir operation on
298 a karst open streamflow hydrological regime: an example from the Dinaric karst (Croatia).
299 *Hydrological Processes*, **24**(26), 3852-3863.

300 Bonacci, O., Trinić, D. & Roje-Bonacci, T. 2008 Analysis of the water temperature regime of the
301 Danube and its tributaries in Croatia. *Hydrological Processes*, **22**(7), 1014-1021.

302 Chen, D., Hu, M., Guo, Y. & Dahlgren, R. A. 2016 Changes in river water temperature between
303 1980 and 2012 in Yongan watershed, eastern China: magnitude, drivers and models. *Journal of*
304 *Hydrology*, **533**, 191-199.

305 Cingi, S., Keinänen, M. & Vuorinen, P. J. 2010 Elevated water temperature impairs fertilization and
306 embryonic development of whitefish *Coregonus lavaretus*. *Journal of Fish Biology*, **76**(3), 502-
307 521.

308 Cox, B. A. & Whitehead, P. G. 2009 Impacts of climate change scenarios on dissolved oxygen in
309 the River Thames, UK. *Hydrology Research*, **40**(2-3), 138-152.

310 Deweber, J. T. & Wagner, T. 2014 A regional neural network ensemble for predicting mean daily
311 river water temperature. *Journal of Hydrology*, **517**(2), 187-200.

312 Feng, M., Zolezzi, G. & Pusch, M. 2018 Effects of thermopeaking on the thermal response of alpine
313 river systems to heatwaves. *Science of the Total Environment*, **612**, 1266-1275.

314 Fullerton, A. H., Torgersen, C. E., Lawler, J. J., Steel, E. A., Ebersole, J. L. & Lee, S. Y. 2018
315 Longitudinal thermal heterogeneity in rivers and refugia for coldwater species: effects of scale
316 and climate change. *Aquatic Sciences*, **80**, 3.

317 Hardenbicker, P., Viergutz, C., Becker, A., Kirchesch, V., Nilson, E. & Fischer, H. 2016 Water
318 temperature increases in the river Rhine in response to climate change. *Regional Environmental*
319 *Change*, **17**, 1-10.

320 Isaak, D. J., Wollrab, S., Horan, D. & Chandler, G. 2012 Climate change effects on stream and river
321 temperatures across the northwest U.S. from 1980–2009 and implications for salmonid fishes.
322 *Climatic Change*, **113**(2), 499-524.

323 Kim, J. H., Park, H. J., Hwang, I. K., Han, J. M., Kim, D. H., Oh, C. W., Lee, J. S. & Kang, J. C.
324 2017 Toxic effects of juvenile sablefish, *Anoplopoma fimbria* by ammonia exposure at different
325 water temperature. *Environmental Toxicology and Pharmacology*, **54**, 169-176.

326 Lepori, F., Pozzoni, M. & Pera, S. 2014 What drives warming trends in streams? A case study from
327 the Alpine Foothills. *River Research and Applications*, **31**(6), 663-675.

328 Markovic, D., Scharfenberger, U., Schmutz, S., Pletterbauer, F. & Wolter, C. 2013 Variability and
329 alterations of water temperatures across the Elbe and Danube River Basins. *Climatic Change*,
330 **119**(2), 375-389.

331 Moatar, F. & Gailhard, J. 2006 Water temperature behaviour in the River Loire since 1976 and 1881.
332 *Comptes Rendus Geoscience*, **338**(5), 319-328.

333 Orr, H. G., Simpson, G. L., des Clers, S., Watts, G., Hughes, M., Hannaford, J., Dunbar, M. J., Laiz é

334 C. L. R., Wilby, R. L., Battarbee, R. W. & Evans, R. 2015 Detecting changing river temperatures
335 in England and Wales. *Hydrological Processes*, **29**(5), 752-766.

336 Pekárová P., Miklášek, P., Halmová D., Onderka, M., Pekár, J., Kučárová, K., Liová S. & Škoda,
337 P. 2011 Long-term trend and multi-annual variability of water temperature in the pristine Bela
338 River basin (Slovakia). *Journal of Hydrology*, **400**(3-4), 333-340.

339 Piotrowski, A. P., Napiorkowski, M. J., Napiorkowski, J. J. & Osuch, M. 2015 Comparing various
340 artificial neural network types for water temperature prediction in rivers. *Journal of Hydrology*,
341 **529**(1), 302-315.

342 Rice, K. C. & Jastram, J. D. 2015 Rising air and stream-water temperatures in Chesapeake Bay
343 region, USA. *Climatic Change*, **128**(1-2), 127-138.

344 Toffolon, M. & Piccolroaz, S. 2015 A hybrid model for river water temperature as a function of air
345 temperature and discharge. *Environmental Research Letters*, **10**, 114011.

346 van Vliet, M. T. H., Ludwig, F., Zwolsman, J. J. G., Weedon, G. P. & Kabat, P. 2011 Global river
347 temperatures and sensitivity to atmospheric warming and changes in river flow. *Water*
348 *Resources Research*, **47**(2), 247-255.

349 van Vliet, M. T. H., Franssen, W. H. P., Yearsley, J. R., Ludwig, F., Haddeland, I., Lettenmaier, D.
350 P. & Kabat, P. 2013 Global river discharge and water temperature under climate change. *Global*
351 *Environmental Change*, **23**(2), 450-464.

352 Webb, B. W., Clack, P. D. & Walling, D. E. 2003 Water–air temperature relationships in a Devon
353 river system and the role of flow. *Hydrological Processes*, **17**(15), 3069-3084.

354 Žganec, K. 2012 The effects of water diversion and climate change on hydrological alteration and
355 temperature regime of karst rivers in central Croatia. *Environmental Monitoring and Assessment*,

356 **184**(9), 5705-5723.

357 Zhu, S., Heddam, S., Nyarko, E. K., Hadzima-Nyarko, M., Piccolroaz, S. & Wu, S. 2018 Modeling

358 daily water temperature for rivers: comparison between adaptive neuro-fuzzy inference systems

359 and artificial neural networks models. *Environmental Science and Pollution Research*.

360 <https://doi.org/10.1007/s11356-018-3650-2>